# Supporting Information

## Birkner and Navrotsky 10.1073/pnas.1320014111

### SI Text

**Synthesis.** Nanophase $Mn_2O_3$ was synthesized using a previously reported oxidative precipitation method (1). Under continuous stirring and nitrogen sparging, excess ammonium hydroxide was added dropwise to a Mn(II) nitrate solution until a pH of about 10 was reached. The color changes associated with product formation began with the faint pink of $Mn^{2+}$, proceeded through pale golden yellow on initial addition of ammonium hydroxide, and then turned the color of café latte until, finally, the color of hot cocoa developed. Still continuing to stir the reaction matrix, but ceasing the nitrogen sparging, the reaction vessel was then closed using a screw cap. The precipitates were allowed to continue reacting/aging for 6 h. The silty-fine, light-medium brown precipitate was washed by repeated centrifugation and addition of fresh, cool (10–15 °C) nitrogen-sparged ultrapure water, until extraneous ions had been removed as evidenced by 0.14 mS conductivity of the final rinsate. The washed solids were vacuum dried, followed by gentle grinding by mortar and pestle into powder to maximize surface exposure as well as to produce an easily managed fine powder for experiments. The light-medium brown powder was then annealed in a covered platinum crucible at 700 °C for 2 h under a ramping program of 10 °C/min. The final product is a medium brown powder, like a very fine-grained instant coffee. The observed color changes from initial solution to final product were a very useful indication of proper reaction progress and therefore have been described in detail above. This synthesis method produced grams of sample, which allowed all experiments to be carried out using the same batch. The product was identified as bixbyite ($Mn_2O_3$) as shown in the X-ray pattern in Fig. S2.

**Characterization.** ***Powder X–ray diffraction.*** All phases were analyzed using a Bruker AXS D8 Advance diffractometer (Cu Kα radiation, 1.540596 Å) operated at 45 kV and 40 mA. The powder X-ray diffraction patterns were collected at room temperature (25 °C) using a step size of 0.02 °2θ and 10-s dwell time. Peak profiles were fitted with a pseudo-Voigt function. International Center for Diffraction Data (ICDD) reference patterns were used in conjunction with analysis performed with Jade software (version 6.11, 2002; Materials Data Inc.) to evaluate the phases or phase mixtures present, their amounts, lattice parameters, and estimated crystallite sizes using the Scherrer equation (2, 3). The identified $Mn_2O_3$ corresponded to ICDD file number 41-1442 (4) and $Mn_3O_4$ to ICDD file number 80-0382 (5).

***Specific surface area analysis.*** Adsorption isotherms of nitrogen at −196 °C (liquid nitrogen temperature) were measured using an ASAP 2020 (Micromeritics) static volumetric apparatus in the $P/P_0$ range 0.05–0.3. Before measurements, the samples were outgassed at room temperature under turbomolecular pump vacuum after which the temperature was increased at 10 °C/min to 350 °C and then maintained for 4 h to remove most preadsorbed water without losing phase integrity or surface area. Specific surface area was calculated using a multipoint Brunauer–Emmett–Teller (BET) method (6).

***Thermogravimetric analysis and differential scanning calorimetry.*** The samples were heated to 700 °C at 10 °C/min under a flow of argon (75 mL/min) in platinum crucibles using the Setaram Labsys Evo instrument and associated Calisto software. The thermogravimetric analysis (TGA) data were corrected for buoyancy by running an empty crucible. $H_2O$ content was determined from the weight difference (obtained on a microbalance for highest accuracy) before and after annealing the samples overnight at 700 °C. Before TGA, the samples were equilibrated for 1 mo in the calorimetry suite that maintains a controlled environment for constant temperature (25 °C) and humidity (50%).

***Controlled heating and cooling experiments.*** These experiments used controlled heating to observe changes in the amount of water, phases present, and oxidation states in the samples. The 350 °C procedure used a heating/cooling cycle of 25–350 °C at 10 °C/min, 350 °C for 4 h, 350–25 °C at 10 °C/min. The 700 °C procedure used a heating/cooling cycle of 25–350 °C at 10 °C/min, 350 °C for 4 h, 350–700 °C at 10 °C/min, 700–25 °C at 10 °C/min. Sample heating occurred under evacuation at roughing pump pressure followed by backfilling with nitrogen. These heating experiments did not alter the starting material phase, as shown in Figs. S3 and S4, respectively.

***Manganese average oxidation state.*** Mn average oxidation state was measured by iodometric titration (7). The method titrates iodine produced by the reaction of iodide with dissolved manganese and can be performed at room temperature. The specific details of the titration of Mn(III and IV) oxidation state and calculations are described in detail elsewhere (8).

***Water adsorption calorimetry.*** The enthalpy of water adsorption was measured by calorimetry at room temperature using a Calvet microcalorimeter, coupled with a Micromeritics ASAP 2020 analysis system as described previously (9). Sample mass was determined using a microbalance (using mass by difference) after being placed in one side of a forked tube (silica glass) and degassed under a static vacuum ($<10^{-3}$ Pa) at elevated temperatures to remove most of the water without coarsening the sample. After BET measurements of specific surface area for the sample and free space for the forked tube, the system was reevacuated. Then, a series of accurately controlled doses of water vapor were released into the system at room temperature until $P/P_0$ reached 0.20 (usually about 8–10 doses with 1.5 h equilibration time between doses). The amount of water per dose equaled 1 μmol water vapor per square meter total sample surface. The adsorption heat of each dose generated an exothermic calorimetric peak. The simultaneous record of the amount of adsorbed water and the adsorption enthalpy provided a high-resolution measurement of differential heat of adsorption as a function of surface coverage.

***Preadsorbed water calculation.*** Moles preadsorbed water per 1 mol $Mn_2O_3$ is shown for the samples in Table 1. Preadsorption coverage (9), which is the number of water molecules chemisorbed to a sample surface per square nanometer total sample surface, is computed as follows:

SA($m^2$/g) * (mol $Mn_2O_3$/157.88 g FW) * (E-18 $m^2$/1 $nm^2$) * (mol preadsorbed $H_2O$/mol $Mn_2O_3$) * (6.022 e23 molecules/mol). The results are shown in Table 2.


1. Birkner N, Navrotsky A (2012) Thermodynamics of manganese oxides: Effects of particle size and hydration on oxidation-reduction equilibria among hausmannite, bixbyite, and pyrolusite. *Am Mineral* 97(8-9):1291–1298.
2. Scherrer P (1918) Bestimmung der Grösse und der inneren Struktur von Kolloidteilchen mittels Röntgenstrahlen. *Nachr Ges Wiss Göttingen* 26(2): 98–100.
3. Patterson AL (1939) The Scherrer formula for X-ray particle size determination. *Phys Rev* 56(10):978–982.
4. Geller S (1971) Structures of alpha-$Mn_2O_3$, $(Mn_{0.983}Fe_{0.017})_2O_3$ and $(Mn_{0.37}Fe_{0.63})_2O_3$ and relation to magnetic ordering. *Acta Crystallogr B* 27(4):821–828.
5. Jarosch D (1987) Crystal structure refinement and reflectance measurements of hausmannite. *Mineral Petrol* 37:15–23.

6. Brunauer S, Emmett PH, Teller E (1938) Adsorption of gases in multimolecular layers. *J Am Chem Soc* 60(2):309–319.
7. Murray JW, Balistrieri LS, Paul B (1984) The oxidation state of manganese in marine sediments and ferromanganese nodules. *Geochim Cosmochim Acta* 48(6):1237–1247.
8. Birkner N, et al. (2013) Energetic basis of catalytic activity of layered nanophase calcium manganese oxides for water oxidation. *Proc Natl Acad Sci USA* 110(22):8801–8806.
9. Ushakov SV, Navrotsky A (2005) Direct measurements of water adsorption enthalpy on hafnia and zirconia. *Appl Phys Lett* 87(16):164103.

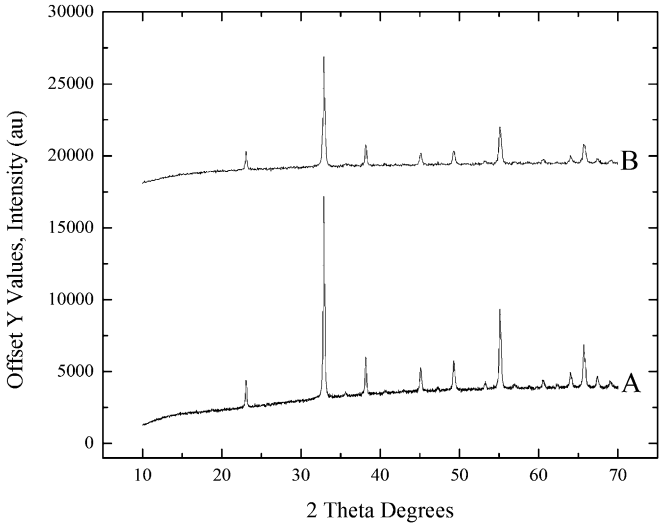


**Fig. S1.** X-ray powder pattern: (*A*) $Mn_2O_3$ sample after synthesis; (*B*) a nanophase $Mn_2O_3$ as reference comparison.

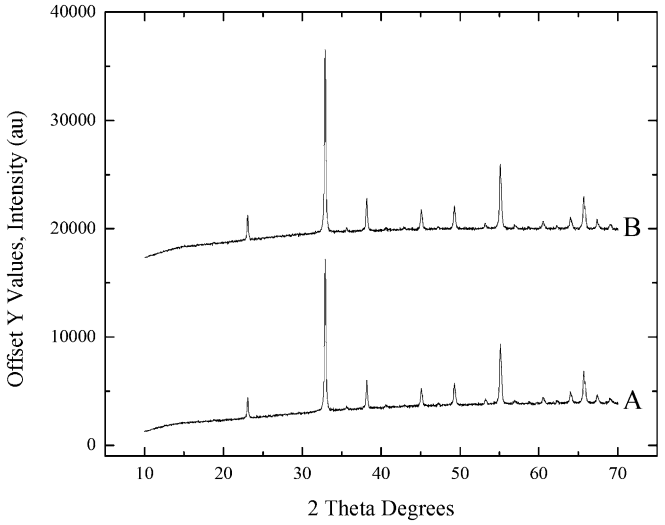


**Fig. S2.** X-ray powder pattern of sample after heating at 350 °C for 4 h: (*A*) $Mn_2O_3$ sample before heating; (*B*) $Mn_2O_3$ sample after heating.

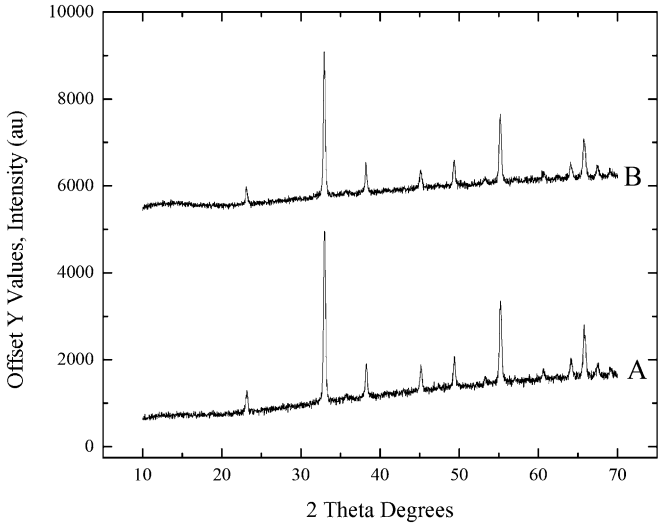


**Fig. S3.** Powder pattern of sample desorbed using our 700 °C procedure: (*A*) $Mn_2O_3$ sample before heating method; (*B*) $Mn_2O_3$ sample after heating method.

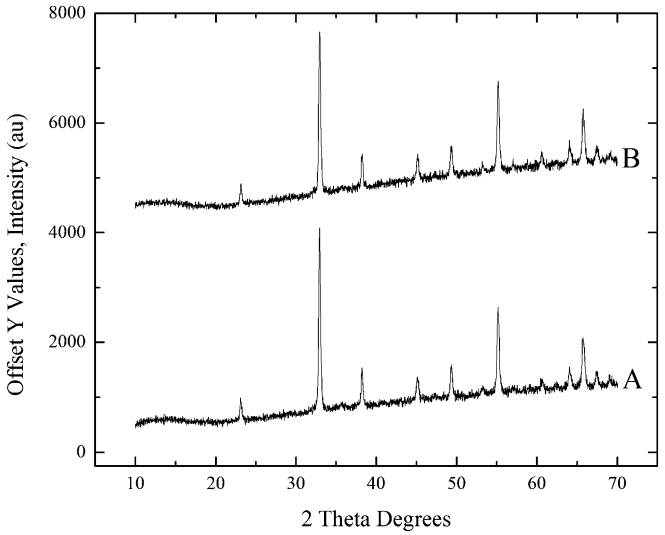


**Fig. S4.** Reversal of phase transformation: (*A*) initial $Mn_2O_3$ before water-adsorption-induced phase transformation; (*B*) $Mn_2O_3$ after room-temperature, water-adsorption-induced phase transformation followed by heat treatment using our 700 °C procedure.

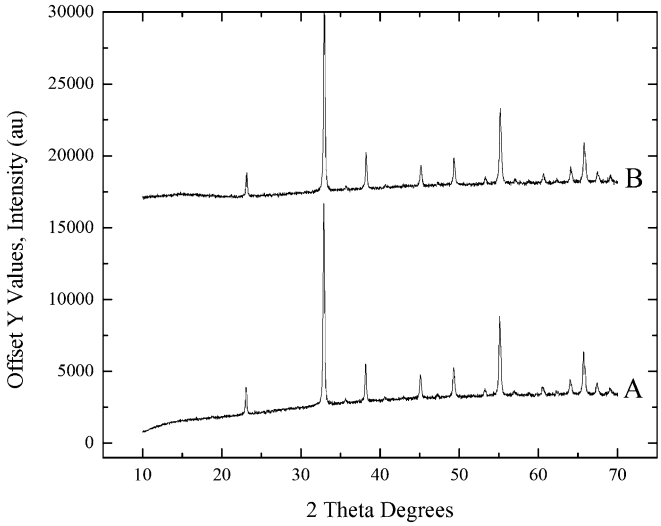


**Fig. S5.** X-ray powder pattern of initially dry sample passivated with 2% total surface coverage with water, equilibrated for 24 h, and then exposed to standard water adsorption. (*A*) $Mn_2O_3$ sample before treatment; (*B*) $Mn_2O_3$ sample after water adsorption treatment of 2% total surface coverage.